Three-Dimensional Axisymmetric Cloak Based on the Cancellation of Acoustic Scattering from a Sphere

L. Sanchis,[1] V. M. García-Chocano,[2] R. Llopis-Pontiveros,[1] A. Climente,[2]
J. Martínez-Pastor,[1] F. Cervera,[2] and J. Sánchez-Dehesa[2,*]

[1]*UMDO (Unidad Asociada al CSIC-IMM), Instituto de Ciencia de Materiales, Universidad de Valencia, P.O. Box 22085, 46071 Valencia, Spain*

[2]*Wave Phenomena Group, Universitat Politècnica de València, Camino de Vera s.n. (Edificio 7F), ES-46022 Valencia, Spain*

(Received 5 August 2012; revised manuscript received 27 November 2012; published 20 March 2013)

This Letter presents the design, fabrication, and experimental characterization of a directional three-dimensional acoustic cloak for airborne sound. The cloak consists of 60 concentric acoustically rigid tori surrounding the cloaked object, a sphere of radius 4 cm. The major radii and positions of the tori along the symmetry axis are determined using the condition of complete cancellation of the acoustic field scattered from the sphere. They are obtained through an optimization technique that combines genetic algorithm and simulated annealing. The scattering cross section of the sphere with the cloak, which is the magnitude that is minimized, is calculated using the method of fundamental solutions. The low-loss fabricated cloak shows a reduction of the 90% of the sphere scattering cross section at the frequency of 8.55 kHz.

DOI: 10.1103/PhysRevLett.110.124301 PACS numbers: 43.20.+g, 43.28.+h, 43.58.+z

Acoustic cloaking is a phenomenon that renders objects undetectable to sound waves [1,2]. Cloaking shells were initially proposed in two dimensions (2D) using acoustic metafluids with anisotropic inertia and scalar bulk modulus [2] or isotropic inertia and anisotropic modulus [3]. Afterwards, the proposal was extended to three dimensions (3D) using metafluids in spherical shells [4,5]. Acoustic cloaking based on the scattering cancellation has also been proposed for an elastic sphere covered by a thin elastic isotropic shell [6]. A hybrid method involving a transformation acoustic conformal map with a scattering cancellation has also been suggested to reduce the scattering cross section of objects in an aqueous environment [7]. Despite the numerous works reporting proposals for making cloaks physically realizable [8,9], only the experiments by Zhang *et al.* [10] and Popa *et al.* [11] claim the demonstration of acoustic cloaking. No practical realizations of 3D cloaks have been reported so far, though, in principle, they can be engineered following the same recipes.

The cloaking of mechanical waves is also receiving increasing interest due to its potential application as vibration isolators. For example, the cloaking of bending waves theoretically proposed by Farhat *et al.* [12] was followed by its experimental demonstration by Stenger *et al.* [13].

In order to design devices that perform a prescribed operation—like acoustic cloaking—there is a powerful method called ''inverse design'' which has been employed to develop a broad variety of devices in optics [14–18] and in acoustics [19,20]. In particular, photonic cloaks based on inverse design have been reported [18,21]. A directional acoustic cloak has been experimentally realized in 2D by García-Chocano *et al.* [20].

This Letter reports the design, construction, and experimental demonstration of a directional axisymmetric acoustic cloak in 3D. It is based on a specific distribution of concentric tori with respect to the sound propagation direction, which crosses the center of the cloaked object—an acoustically rigid sphere. The positions and major radii of the tori surrounding the sphere are determined such that they cancel the field scattered by the sphere. Those parameters are obtained using an optimization tool that combines the genetic algorithm [22] and the simulated annealing [23]. The scattering cross section is the quantity that is minimized in the optimization procedure, and its value is obtained using the method of the fundamental solutions (MFS) [24,25]. It is demonstrated that the designed cloak cancels the field scattered by the bare sphere giving a perfect reconstruction of the incident sound wave front. The cloaking performance of the designed cloak has been proven with a prototype constructed with a 3D printer.

The chosen radius of the sphere is $R_0 = 4$ cm and the prefixed operational frequency of the cloak has been selected with the condition $\lambda = R_0$, which for airborne sound corresponds to the linear frequency $\nu = c_b/R_0 = 8.62$ kHz, where $c_b = 344.8$ m/sec is the phase velocity of air at normal room temperature ($T = 22°$) and normal atmospheric pressure ($P_0 = 0.751$ m Hg) [26]. A set of 60 acoustically rigid tori with equal transversal section with radii $r_t = 0.267$ cm has been employed as the cloaking shell.

The scattering problem defined by the sphere and the tori has been solved by the MFS, which is specially suitable for axisymmetric scatterers [25]. In what follows we give a brief account of its application to calculate the scattering cross section.

Let us consider an incident plane wave that travels along the z axis, $P^{\text{inc}}(z;\omega) = e^{ikz}$, where k is the wave number. The angular frequency, $\omega = 2\pi \times \nu$, is implicitly assumed

in the temporal dependence and will be omitted in the rest of the Letter for simplification. Within the MFS the total scattered pressure can be expressed in cylindrical coordinates as

$$P^{\text{scatt}}(\rho, z) = \sum_{j=1}^{N} \alpha_j G_{\text{axis}}(\rho, z; \rho'_j, z'_j), \tag{1}$$

where N is the total number of virtual ring sources located at positions (ρ'_j, z'_j) with amplitudes α_j, and G_{axis} is the free space axisymmetric Green's function of the corresponding Helmholtz equation [25]; i.e.,

$$G_{\text{axis}}(\rho, z; \rho'_j, z'_j) = (4\pi)^{-1} \int_0^{2\pi} \frac{e^{ikR_j}}{R_j} d\phi, \tag{2}$$

where R_j is the distance between the j source and the point (ρ, z) where the field is calculated [27]; i.e., $R_j^2 = \rho^2 + \rho_j'^2 + (z - z'_j)^2 - 2\rho\rho'_j \cos\phi$, with $\phi = \theta' - \theta$.

N sample points (ρ_i, z_i) are appropriately selected on the surface of the scatterers where we impose the condition that they are acoustically rigid; i.e., the component of the velocity normal to the surface must be zero, $|\partial P^{\text{total}}/\partial n|_{(\rho_i, z_i)} = 0$, with $\vec{n}$ indicating the normal to the surface at the given sample point. In this manner we arrive at the following linear system of coupled equations:

$$\left[\frac{\partial P^{\text{inc}}}{\partial n}\right]_{(\rho_i, z_i)} + \sum_{j=1}^{N} \alpha_j \left[\frac{\partial G_{\text{axis}}}{\partial n}\right]_{(\rho_i, z_i)} = 0, \quad i = 1, \ldots, N, \tag{3}$$

where the coefficients α_j are the unknowns.

Once the multiple scattering problem is solved and the α coefficients are obtained, the scattering cross section by the sphere with the cloak σ_c is obtained using the optical theorem [27],

$$\sigma_c(\omega) = \frac{2\pi}{k} \text{Im}\left[\sum_{j=1}^{N} \alpha_j e^{-ikz_j}\right]. \tag{4}$$

In order to get the distribution of tori that conceal the central sphere at the prefixed frequency ω_0, we choose as the fitness function

$$F = 1 - \frac{\sigma_c(\omega_0)}{\sigma_{\text{sph}}(\omega_0)}, \tag{5}$$

where $\sigma_{\text{sph}}(\omega_0)$ is the cross section of the bare sphere. After optimization, $\sigma_c(\omega_0)$ takes its minimum value. Therefore, $F = 1$ defines the condition of complete acoustic concealment.

The 3D scattering algorithm described above is employed as the direct solver providing a fast and accurate calculation of the fitness function [see Eq. (5)] of both structures, the bare sphere and the sphere with the cloak.

The optimization procedure starts with the tori homogeneously distributed along the z axis with their planes perpendicular to it. The dimension and position of each torus along the axis are calculated making use of two optimization methods, the genetic algorithm and simulated annealing. In brief, the binary-coded genetic algorithm operates on a population of candidate structures in order to produce the new ones with better performance in an iterative process inspired by Darwinian evolution [22]. On the other hand, the simulated annealing is an optimization method inspired by a process of slowly cooling a molten metal in order to obtain a uniform crystalline structure with a state of minimum energy [23].

Figure 1(a) shows an artistic representation of the sphere surrounded by the tori obtained after optimization. It is observed that the spatial distribution of the tori is not uniform along the z axis and has a mirror symmetry plane passing through the origin of coordinates, $z = 0$. The fitness function of this optimum structure has a value $F = 0.978$.

The calculated field maps for the sphere with and without the cloak are depicted in Fig. 2, where it is observed that the shadowing produced by the rigid sphere is almost completely restored when it is surrounded by the set of tori. Let us remark that the cloaking performance described in Fig. 2(b) can be understood as a destructive interference effect between the waves scattered by the sphere and the cloak, respectively. For the case of the sphere with the cloak, a strong accumulation of field pressure near the sphere surface is seen. This effect represents a resonant mode that appears as a consequence of the multiple scattering interference phenomenon. The robustness of the cloaking

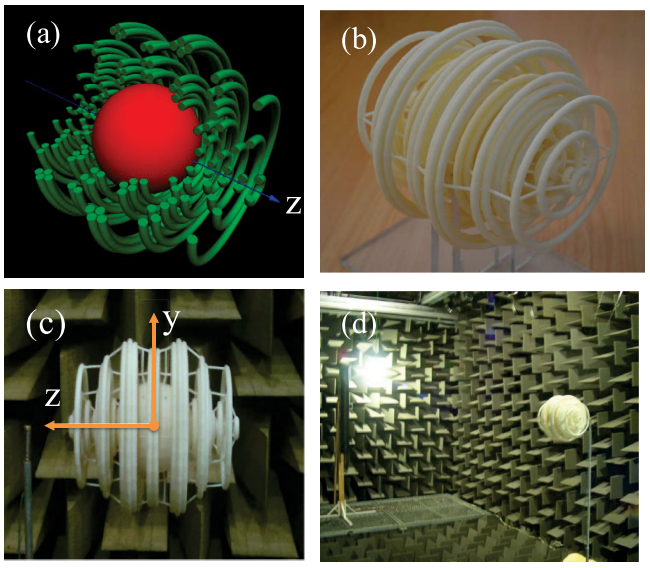

FIG. 1 (color online). (a) Schematic representation of the 3D designed cloak. The cloak consists of 60 concentric tori surrounding the central spherical object. (b) Photograph of the cloak taken after its fabrication. It is made in plastic with a central sphere of radius 4 cm. The total length of the sample (object + cloak) along the z axis is 17 cm. (c),(d) Photographs taken inside the anechoic room.

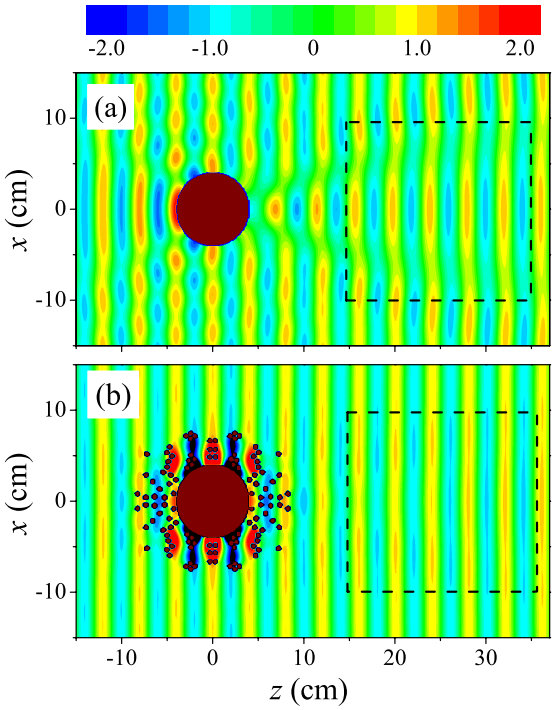

FIG. 2 (color online). (a) Map of the total pressure (real part in arbitrary units) obtained from the scattering of an incident plane wave with frequency 8.62 kHz with a rigid sphere with radius 4 cm. (b) Map corresponding to the sphere surrounded by the designed cloak. Both maps are calculated using a multiple scattering approach based on the method of fundamental solutions. The rectangle defined by the dashed lines represents the area scanned by the experimental setup.

performance as a function of various effects is described in the Supplemental Material [27].

To support experimentally the previous findings, a sphere of radius 4 cm and the sphere with the cloak were fabricated using a commercial 3D printer. A photo of the sphere with the cloak after its fabrication is shown in Fig. 1(b), where it is noticeable how the tori are linked by thin beams in order to keep fixed their calculated positions. The material employed in the construction of the prototype is acoustically rigid in the range of frequencies explored.

The sphere with and without the cloak, respectively, was separately characterized in an anechoic chamber with dimensions $8 \times 6 \times 3$ m^3. The incident sound is excited using a column speaker aligned with the axis of the cloak [see Figs. 1(c) and 1(d)]. Two linear stages are used to move a B&K 4958 microphone that performs a 2D sweep inside the chamber. The robot scans an area behind the samples of 20×20 cm^2 in the horizontal XZ plane with a spatial resolution of 0.5 cm in each direction. This area is represented in Fig. 2 by the rectangle defined with dashed lines. An area with the same dimensions and spatial resolution is scanned in the vertical YZ plane. A chirp consisting of a frequency sweep between 7.5 and 9.5 kHz has been used as an excitation signal. It is emitted at each spatial position of the moving robot until the pressure is acquired by the microphone. The received signal is processed through a fast Fourier transform which provides its amplitude and phase. In order to reduce the presence of random noise, several emissions are performed and the acquired responses are averaged.

A series of measurements around the prefixed operational frequency were performed in order to quantify the scattering reduction of the sphere with the cloak. Figure 3 shows the pressure maps measured at 8.55 kHz, which is the resulting frequency at which the averaged visibility of the object with cloak takes the minimum value. This optimum frequency is slightly different to 8.62 kHz, which was the frequency prefixed for cancellation. The small discrepancy comes from the fact that the sound speed inside the anechoic chamber is 344.17 m/sec , corresponding to an average temperature of 21.63 °C with humidity of 54.7% [26].

Figure 3 shows the real part of the total pressure measured in the area of exploration belonging to the horizontal plane (left-hand panels) and vertical plane (right-hand panels). The spectra taken in free space show some wiggling in the wave fronts that was originated from unwanted

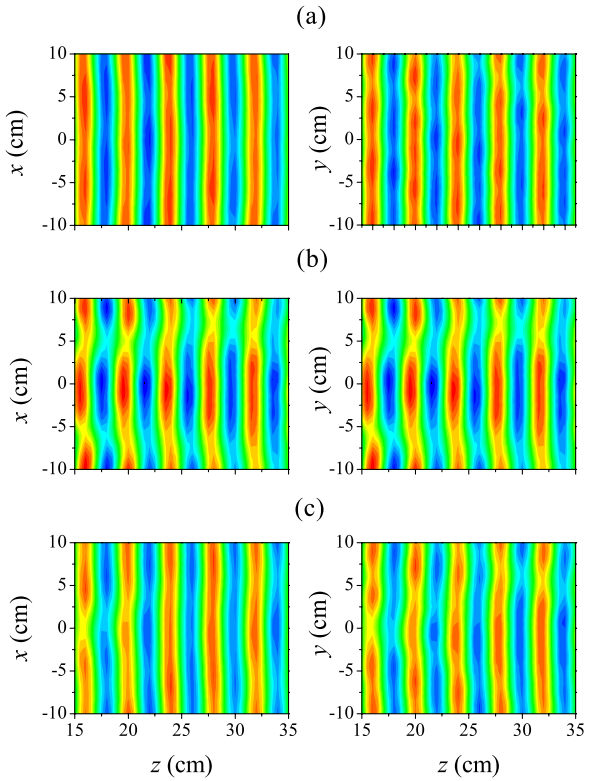

FIG. 3 (color online). Pressure maps measured at 8.55 kHz, the operational frequency of the fabricated cloak. Maps on the left (right) represent the real part of the total pressure on the horizontal (vertical) plane. (a) Free space, (b) bare sphere, (c) sphere + cloak.

reflections in the free-echo chamber. These reflections are due to the high working frequency of the designed cloak together with the presence of the components of the experimental setup; some of them have sizes of the order of the wavelength employed in the experiments (a few cm). The spectra of the bare sphere in Fig. 3(b) clearly show the shadowing by the diffracted sound. This shadowing is substantially smaller than that observed for a 2D cylinder [20]. Finally, the spectra with the cloak [see Fig. 3(c)] show that the plane wave fronts are reconstructed but with the limitations already observed in the free space spectra. It is important to remark that all the maps are represented with the same color scale, which means that no appreciable losses can be associated with the performance of the cloak.

The averaged visibility of an object γ is a parameter employed to characterize the cloaking performance. It is a frequency dependent function that is defined as [10]

$$\gamma(\omega) = \frac{1}{N}\sum_{j}\frac{|P_{\max,j}| - |P_{\min,j}|}{|P_{\max,j}| + |P_{\min,j}|}, \qquad (6)$$

where $P_{\max,j}$ and $P_{\min,j}$ are the maximum and minimum peak values along a given wave front j, and N is the total number of wave fronts explored (see Fig. 3).

The averaged visibility can be compared to the traditional measurement of scattering cross section, but performed for the convenience of the field measurement available in our experimental setup. The upper panels in Fig. 4 plot the average visibility of the cloaked sphere γ_c over all the wave fronts on the transmitted side and compared with that of the bare sphere γ_{sph}. The results obtained for both the horizontal and the vertical planes are depicted. The visibility for the free space γ_0 when there is neither sphere nor cloak is also plotted and is employed as a reference in our setup. The measured visibilities (symbols) are compared with those (lines) derived from simulations using the method of fundamental solutions. Note that the reference visibility (black triangles) that is the visibility for a propagating plane wave in free space, which should be zero, is spoiled by the presence of unwanted scattering events inside the chamber. However, it is observed that the data follow fairly well the trend of the numerical simulations. At 8.55 kHz we can read the visibility of 0.25 for the bare sphere whereas the visibility of the cloaked sphere is reduced to 0.10, a value very close to 0.07, which is the one measured in free space. This result confirms the strong reduction of the shadowing observed in the pressure map plot in Fig. 3(c).

The lower panels in Fig. 4 show a comparison between the experimentally determined ratio $\gamma_c/\gamma_{\text{sph}}$ (symbols) and the ratio between cross sections $\sigma_c/\sigma_{\text{sph}}$ (black line). The last one is obtained from numerical simulations employing the method of fundamental solutions [27]. The visibilities are taken with respect to the reference visibility for a fair comparison. It is observed that the ratio $\gamma_c/\gamma_{\text{sph}}$ effectively gives a good representation of $\sigma/\sigma_{\text{sph}}$ for the frequencies near the one employed as the target in the cancellation procedure. For smaller or higher frequencies the ratio $\gamma_c/\gamma_{\text{sph}}$ does not necessarily account for the strong perturbations produced by the backscattered field. These panels demonstrate the 3D performance of our cloak. A 90% of maximum reduction of the sphere cross section is experimentally obtained at 8.55 kHz. The cloak bandwidth is 120 Hz. This bandwidth has been established using the convention [10] that, for any frequency enclosed by the bandwidth, a scattering reduction larger than 70% should be measured [27].

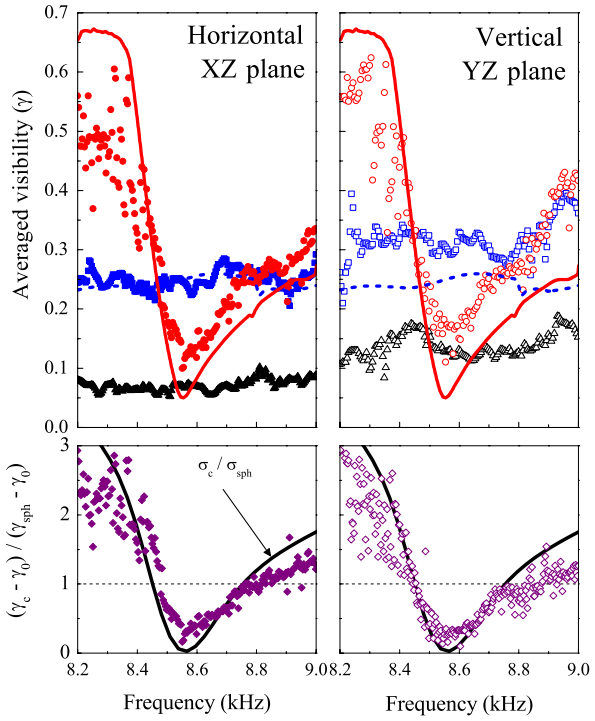

FIG. 4 (color online). Upper panels: Plot of the averaged visibility (γ) as a function of the frequency. The experimental results with and without the cloak are marked by red circles and blue squares, respectively. The reference visibility (γ_0) when there is no object is marked by black triangles. The lines represent the simulations. Lower panels: The purple diamonds plot the ratio between the averaged visibility of the sphere with the cloak (γ_c) and without cloak (γ_{sph}). Both are shifted by the reference visibility. The black lines represent the ratio between the scattering cross sections of the sphere with and without cloak, $\sigma_c/\sigma_{\text{sph}}$, obtained from simulations. Full (empty) symbols define data on the horizontal (vertical) plane.

In summary, we have demonstrated a low-loss 3D cloak that can reduce the visibility of the hidden object for airborne sound waves. It has been obtained from the condition of the total cancellation of the waves scattered by a sphere at a prefixed frequency. This result can be considered as the acoustic analogue of the recently proposed cloaking structures based on scattering cancellation of electromagnetic waves [28]. The fabricated cloak consists of 60 acoustically rigid tori that at 8.55 kHz suppresses up to 90% of the waves scattered by the sphere. Though the cloak is

directional and narrow banded, there are several possibilities for its improvement using additional parameters. For example, a broadband operation could be made by imposing the cancellation over several frequencies. Designing an omnidirectional cloak could also be possible by performing a multiobjective optimization [16]. Moreover, cloaks for underwater operation could also be feasible by including the elasticity of the tori employed in their design.

This work is partially supported by the Spanish Ministerio de Economía y Competitividad under Contracts No. TEC2010-19751, No. TEC2011-29120-C05-01, and No. CSD2008-00066 (CONSOLIDER Program), and by the U.S. Office of Naval Research. The authors acknowledge the "Centro de Tecnologías Físicas" at the UPV for technical help during data acquisition. We also acknowledge the computing facilities provided by the Universidad de Valencia.

*Corresponding author.
jsdehesa@upv.es

[1] G. W. Milton, M. Briane, and J. R. Willis, New J. Phys. **8**, 248 (2006).
[2] S. A. Cummer and D. Schurig, New J. Phys. **9**, 45 (2007).
[3] A. N. Norris, J. Acoust. Soc. Am. **125**, 839 (2009).
[4] H. Y. Chen and C. T. Chan, Appl. Phys. Lett. **91**, 183518 (2007).
[5] S. A. Cummer, B. I. Popa, D. Schurig, D. R. Smith, J. Pendry, M. Rahm, and A. Starr, Phys. Rev. Lett. **100**, 024301 (2008).
[6] M. D. Guild, A. Alú, and M. R. Habermann, J. Acoust. Soc. Am. **129**, 1355 (2011).
[7] T. P. Martin and G. J. Orris, Appl. Phys. Lett. **100**, 033506 (2012).
[8] D. Torrent and J. Sánchez-Dehesa, New J. Phys. **10**, 063015 (2008).
[9] Y. Cheng, F. Yang, J. Y. Xu, and X. J. Liu, Appl. Phys. Lett. **92**, 151913 (2008).
[10] S. Zhang, C. Xia, and N. Fang, Phys. Rev. Lett. **106**, 024301 (2011).
[11] B. I. Popa, L. Zigoneanu, and S. A. Cummer, Phys. Rev. Lett. **106**, 253901 (2011).
[12] M. Farhat, S. Guenneau, and S. Enoch, Phys. Rev. Lett. **103**, 024301 (2009).
[13] N. Stenger, M. Wilhelm, and M. Wegener, Phys. Rev. Lett. **108**, 014301 (2012).
[14] L. Sanchis, A. Håkansson, D. López-Zanón, J. Bravo-Abad, and J. Sánchez-Dehesa, Appl. Phys. Lett. **84**, 4460 (2004).
[15] S. Preble, M. Lipson, and H. Lipson, Appl. Phys. Lett. **86**, 061111 (2005).
[16] A. Håkansson, H. T. Miyazaki, and J. Sánchez-Dehesa, Phys. Rev. Lett. **96**, 153902 (2006).
[17] L. Sanchis, M. J. Cryan, J. Pozo, I. J. Craddock, and J. G. Rarity, Phys. Rev. B **76**, 045118 (2007).
[18] J. Andkajaer and O. Sigmund, Appl. Phys. Lett. **98**, 021112 (2011).
[19] A. Håkansson, F. Cervera, and J. Sánchez-Dehesa, Appl. Phys. Lett. **86**, 054102 (2005).
[20] V. M. García-Chocano, L. Sanchis, A. Díaz-Rubio, J. Martínez-Pastor, F. Cervera, R. Llopis-Pontiveros, and J. Sánchez-Dehesa, Appl. Phys. Lett. **99**, 074102 (2011).
[21] A. Håkansson, Opt. Express **15**, 4328 (2007).
[22] D. E. Goldberg, *Genetic Algorithms in Search, Optimization and Learning* (Addison-Wesley, Reading, MA, 1989).
[23] S. Kirkpatrick, C. D. Gelatt, Jr., and M. P. Vecchi, Science **220**, 671 (1983).
[24] A. F. Seybert, B. Soenarko, F. J. Rizzo, and D. J. Shippy, J. Acoust. Soc. Am. **80**, 1241 (1986).
[25] A. Karageorghis and G. Fairweather, J. Acoust. Soc. Am. **104**, 3212 (1998).
[26] Leo L. Beranek, *Acoustics* (Acoustical Society of America, New York, 1996), p. 10.
[27] See Supplemental Material at http://link.aps.org/supplemental/10.1103/PhysRevLett.110.124301 for a thorough discussion on the mathematical procedure.
[28] G. W. Milton and N.-A. P. Nicorivici, Proc. R. Soc. A **462**, 3027 (2006).